

Synthesis, Photophysics, and Transient Absorption Spectroscopic Studies of Luminescent Copper(I) Chalcogenide Complexes. Crystal Structure of $[\text{Cu}_4(\mu\text{-dtpm})_4(\mu_4\text{-S})](\text{PF}_6)_2$ {dtpm = Bis[bis(4-methylphenyl)phosphino]methane}

Vivian Wing-Wah Yam,* Kenneth Kam-Wing Lo, Chun-Ru Wang, and Kung-Kai Cheung

Department of Chemistry, The University of Hong Kong, Pokfulam Road, Hong Kong

Received: November 25, 1996; In Final Form: February 21, 1997[⊗]

A luminescent copper(I) sulfido cluster $[\text{Cu}_4(\mu\text{-dtpm})_4(\mu_4\text{-S})](\text{PF}_6)_2$ (**3**) {dtpm = bis[bis(4-methylphenyl)phosphino]methane} has been synthesized and characterized by X-ray crystallography. Its photophysical and electrochemical properties have also been studied. The long-lived photoluminescence of **3** is assigned to originate from an excited state with a parentage of large ligand-to-metal charge-transfer LMCT $[(\text{S}^{2-}) \rightarrow \text{Cu}_4]$ character, with mixing of metal-centered MC $[(\text{ds}/\text{dp}) \text{Cu}(\text{I})_4]$ state. The phosphorescent state of **3**, as well as those of its analogues $[\text{Cu}_4(\mu\text{-dppm})_4(\mu_4\text{-S})](\text{PF}_6)_2$ (**1**) and $[\text{Cu}_4(\mu\text{-dppm})_4(\mu_4\text{-Se})](\text{PF}_6)_2$ (**2**), have been found to undergo facile electron-transfer reactions with different pyridinium acceptors, which have been investigated with nanosecond transient absorption spectroscopy. Crystal data for **3**: $a = 37.38(1)$ Å, $b = 15.905(7)$ Å, $c = 27.761(5)$ Å, $\beta = 128.69(1)^\circ$, $V = 12881(6)$ Å³, $Z = 4$.

Introduction

It has been well-known that polynuclear d^{10} complexes such as those of copper(I), silver(I), and gold(I) possess remarkable photophysical and photochemical properties.^{1–9} Recently, we have reported a novel class of luminescent tetranuclear d^{10} complexes containing an unsubstituted μ_4 -bridging chalcogenide ligand, $[\text{M}_4(\mu\text{-dppm})_4(\mu_4\text{-E})]^{2+}$ ($\text{M} = \text{Cu},^{9\text{a,b}} \text{Ag};^{9\text{c}} \text{E} = \text{S}, \text{Se}, \text{Te}$). These complexes have been found to exhibit long-lived phosphorescence; the excited states of which have been assigned as an admixture of ligand-to-metal charge-transfer LMCT $[(\text{E}^{2-}) \rightarrow \text{M}_4]$ and metal-centered MC ($d\text{-s}/d\text{-p}$) Cu(I) or Ag(I) character, supported by spectroscopic studies, and Fenske–Hall^{9d} and *ab initio*^{9e} molecular orbital calculations.

In this paper, we report the synthesis, X-ray crystal structure and photophysical properties of a related copper(I) sulfido cluster $[\text{Cu}_4(\mu\text{-dtpm})_4(\mu_4\text{-S})](\text{PF}_6)_2$ (**3**) {dtpm = bis[bis(4-methylphenyl)phosphino]methane}. The long-lived phosphorescent state of the clusters has been found to be strongly reducing and undergo facile electron-transfer quenching with a series of pyridinium acceptors.^{9a,b} Direct spectroscopic evidence for the mechanism of these photoredox reactions has been provided by nanosecond transient absorption spectroscopic studies using the complexes $[\text{Cu}_4(\mu\text{-dppm})_4(\mu_4\text{-S})](\text{PF}_6)_2$ (**1**), $[\text{Cu}_4(\mu\text{-dppm})_4(\mu_4\text{-Se})](\text{PF}_6)_2$ (**2**), and $[\text{Cu}_4(\mu\text{-dtpm})_4(\mu_4\text{-S})](\text{PF}_6)_2$ (**3**) {dppm = bis(diphenylphosphino)methane; dtpm = bis[bis(4-methylphenyl)phosphino]methane}.

Experimental Section

Materials. Sodium sulfide hydrate (GR) was obtained from Merck and was used as received. Tris(4-methylphenyl)phosphine,^{10a} $[\text{Cu}(\text{CH}_3\text{CN})_4]\text{PF}_6$,^{10b} and $[\text{Cu}_4(\mu\text{-dppm})_4(\mu_4\text{-E})](\text{PF}_6)_2$ [$\text{E} = \text{S}$ (**1**),^{9a} Se (**2**)^{9b}] were prepared by published procedures.

The pyridinium salts for transient absorption spectroscopic studies were prepared by refluxing the substituted pyridines with the corresponding alkylating reagent in acetone–ethanol (1:1 v/v) for 4 h, followed by metathesis in water using ammonium hexafluorophosphate and subsequent recrystallization from

acetonitrile–diethyl ether. Tetra-*n*-butylammonium hexafluorophosphate was purchased from Aldrich Chemical Co. and was recrystallized three times from hot ethanol and then dried under vacuum at 110 °C for 24 h. THF, CH_2Cl_2 , and CH_3CN were purified by standard procedures.^{10c}

In electrochemical measurements, double-distilled water was used for rinsing throughout the work. All other solvents and reagents were of analytical grade and were used as received. All reactions were carried out in an atmosphere of nitrogen under standard Schlenk conditions.

Preparation of dtpm. It was prepared by modification of a reported method for dppm synthesis.^{10d} To tris(4-methylphenyl)phosphine (7.32 g, 24.0 mmol) in anhydrous THF (50 mL) was added lithium metal strips (0.33 g, 48.0 mmol). The suspension turned deep red within 5 min. After being stirred at room temperature for 24 h, the mixture was filtered to remove any unreacted lithium. 2-Chloro-2-methylpropane (1.61 mL, 24.0 mmol) in 5 mL of THF was added to the solution dropwise to remove the 4-methylphenyllithium. Dichloromethane (0.77 mL, 12.0 mmol) in 10 mL of THF was then added dropwise. The solution was refluxed for 30 min. After workup and recrystallization from $\text{CH}_2\text{Cl}_2/\text{EtOH}$, dtpm was obtained as white needles (1.94 g, 4.4 mmol, 37% yield). ¹H NMR (300 MHz, CDCl_3 , 298 K, relative to TMS) δ 2.3 (s, 12H, methyl H's), 2.7 (m, 2H, methylene H's), 7.1–7.3 (m, 16H, phenyl H's). ³¹P{¹H} NMR (202 MHz, acetone-*d*₆, 298 K, relative to 85% H_3PO_4) δ –24.1 (s). EI-MS m/z at 440 $\{\text{M}\}^+$.

Preparation of $[\text{Cu}_2(\mu\text{-dtpm})_2(\text{CH}_3\text{CN})_2](\text{PF}_6)_2$. It was prepared by modification of the method for the synthesis of $[\text{Cu}_2(\text{dppm})_2(\text{CH}_3\text{CN})_2](\text{PF}_6)_2$.^{10e} $[\text{Cu}(\text{CH}_3\text{CN})_4]\text{PF}_6$ (266.0 mg, 0.714 mmol) and dtpm (314.0 mg, 0.714 mmol) were stirred in 30 mL of CH_2Cl_2 under nitrogen for 4 h. The solution was then filtered and concentrated. Subsequent recrystallization from $\text{CH}_2\text{Cl}_2/\text{diethyl ether}$ gave the product, isolated as white crystals (458.0 mg, 0.332 mmol, 93% yield). ¹H NMR (300 MHz, CD_3CN , 298 K, relative to TMS) δ 2.3 (s, 24H, methyl H's), 3.2 (m, 4H, methylene H's), 6.9–7.1 (m, 32H, phenyl H's). ³¹P{¹H} NMR (202 MHz, CD_3CN , 298 K, relative to 85% H_3PO_4) δ –13.2 (s). Positive FAB-MS m/z at 1006 $\{[\text{Cu}_2(\text{dtpm})_2]\}^+$.

[⊗] Abstract published in *Advance ACS Abstracts*, May 15, 1997.

Preparation of [Cu₄(μ-dtpm)₄(μ₄-S)](PF₆)₂ (3). The preparation was similar to that for the dppm counterpart, **1**. To a solution of [Cu₂(μ-dtpm)₂(CH₃CN)₂](PF₆)₂ (97.0 mg, 0.070 mmol) in acetone (5 mL) was added dropwise a methanolic solution (2 mL) of sodium sulfide hydrate (8.44 mg, 0.035 mmol). The solution turned immediately to yellow and finally orange. Diffusion of diethyl ether vapor into a concentrated acetone solution of the complex afforded [Cu₄(μ-dtpm)₄(μ₄-S)](PF₆)₂ as air-stable orange crystals (70.0 mg, 0.030 mmol, 85% yield). Elemental anal. found (%): C 60.03, H 5.58, P 12.80. Calcd for [Cu₄(dtpm)₄(S)](PF₆)₂·(CH₃)₂CO·CH₃CH₂OCH₂CH₃ (%): C 59.80, H 5.55, P 12.54. ¹H NMR (300 MHz, acetone-*d*₆, 298 K, relative to TMS) δ 2.3 (s, 48H, methyl H's), 3.5 (m, 8H, methylene H's), 7.0–7.3 (m, 64H, phenyl H's). ³¹P{¹H} NMR (202 MHz, acetone-*d*₆, 298 K, relative to 85% H₃PO₄) δ –13.7 (s). Positive FAB-MS *m/z* at 1022 {[Cu₄(dtpm)₄(S)]²⁺, 2189 {[Cu₄(dtpm)₄(S)](PF₆)⁺}. UV/vis (CH₃CN), λ/nm (ε_{max}/dm³ mol⁻¹ cm⁻¹) 272 sh (49,645), 362 sh (4,175), 430 sh (930).

Physical Measurements and Instrumentation. ¹H and ³¹P NMR spectra were recorded on a Bruker DPX-300 (300 MHz) or DRX-500 (500 MHz) FT-NMR spectrometer. All mass spectra were recorded on a Finnigan MAT95 mass spectrometer. Elemental analysis was performed by the Butterworth Laboratories Ltd.

Cyclic voltammetric measurements were carried out by using a Princeton Applied Research (PAR) universal programmer (Model 175) and potentiostat (Model 173). Electrochemical measurements were performed in acetonitrile solutions (0.1 mol dm⁻³ nBu₄NPF₆) with Ag/AgNO₃ (0.1 mol dm⁻³ in CH₃CN) as the reference electrode. The ferrocenium/ferrocene couple (FeCp₂^{+/0}) was used as the internal reference. The working electrode was a glassy carbon (Atomergic Chemetal V25) electrode with a piece of platinum gauze as the counter electrode in a compartment separated from the working electrode by a sintered glass.

Electronic absorption spectra were recorded on a Hewlett-Packard 8452A diode array spectrophotometer. Steady-state emission and excitation spectra recorded at room temperature and 77 K were obtained on a Spex Fluorolog-2 Model F 111 fluorescence spectrophotometer. All solutions for photophysical studies were prepared under high vacuum in a 10 cm³ round-bottomed flask equipped with a sidearm 1-cm fluorescence cuvette and sealed from the atmosphere by a Rotaflo HP6/6 quick-release Teflon stopper. Solutions were rigorously degassed with no fewer than four successive freeze–pump–thaw cycles. Solid-state photophysical measurements were carried out with solid samples loaded in a quartz tube inside a quartz-walled optical Dewar flask. Liquid nitrogen was placed into the Dewar flask for low temperature (77 K) solid-state photophysical measurements. Luminescence quantum yields were measured by the optical dilute method developed by Demas and Crosby.¹¹ Quinine sulfate in 1.0 N H₂SO₄ solution (Φ = 0.546, excitation wavelength at 365 nm) was used as the standard solution.

Emission-lifetime measurements were performed using a conventional laser system. The excitation source was the 355-nm output (third harmonic) of a Quanta-Ray Q-switched GCR-150-10 pulsed Nd:YAG laser. Luminescence decay signals from a Hamamatsu R928 photomultiplier tube were converted to voltage changes by connecting a 50 Ω load resistor and were then recorded on a Tektronix Model TDS 620A digital oscilloscope. Solution samples for luminescence lifetime measurements were degassed by no fewer than four successive freeze–pump–thaw cycles.

TABLE 1: Crystal and Structure Determination Data for 3

formula	[Cu ₄ SP ₈ C ₁₁₆ H ₁₂₀] ²⁺ 2PF ₆ ⁻ ·2(C ₂ H ₅) ₂ O·(CH ₃) ₂ CO
<i>M_r</i>	2544.51
<i>T</i> , K	301
<i>a</i> , Å	37.38(1)
<i>b</i> , Å	15.905(7)
<i>c</i> , Å	27.761(5)
β, deg	128.69(1)
<i>V</i> , Å ³	12881(6)
cryst color and shape	yellow prism
cryst syst	monoclinic
space group	C2/c (No. 15)
<i>Z</i>	4
<i>F</i> (000)	5288
<i>D_c</i> , g cm ⁻³	1.312
cryst dimens, mm	0.25 × 0.20 × 0.35
λ, Å (graphite monochromated, Mo Kα)	0.71073
μ, cm ⁻¹	8.58
colln range	2θ _{max} = 45° (<i>h</i> : 0 to 40; <i>k</i> : 0 to 17; <i>l</i> : –23 to 23)
scan mode; scan speed, deg min ⁻¹	ω–2θ; 16
scan width, deg	0.68 + 0.35 tan θ
no. of data coll'd	8939
no. of unique data	8777
no. of data used in refinement, <i>m</i>	4735
no. of params refined, <i>p</i>	643
<i>R^a</i>	0.060
<i>R_w^a</i>	0.079
goodness-of-fit, <i>S</i>	2.57
max shift, (Δ/σ) _{max}	0.04 (for the cation)
residual extrema in final diff map, e Å ⁻³	+1.11, –0.56

^a *w* = 4*F*_o²/σ²(*F*_o²), where σ²(*F*_o²) = [σ²(*I*) + (0.028 *F*_o²)²] with *I* > 3σ(*I*).

The optical arrangements for transient absorption spectroscopic and kinetic measurements consist of a linear monitoring beam passing through an absorption cell with photolysis light irradiating the cell normally. Excitation was achieved with the laser system described above. Transient absorption signals were recorded by a photomultiplier tube connected to a 50 Ω load resistor and amplified by a Tektronix AM502 differential amplifier (<1 MHz) which was then digitized with a Tektronix TDS 620A digital oscilloscope, interfaced to an IBM-compatible personal computer for data treatment. Transient absorption spectra of the photolyzed solutions were measured perpendicular to the laser beam with a 250 W quartz–tungsten–halogen (QTH) lamp as the monitoring light source. The entire optical difference spectrum was generated by the point-to-point method through the selection of wavelength of the monitoring monochromators.

Crystal Structure Determination. Single crystals of **3** were obtained from slow diffusion of diethyl ether vapor into a concentrated acetone solution of the complex. Diffraction data were collected at 298 K on a Rigaku AFC7R diffractometer with graphite monochromatized Mo Kα radiation (λ = 0.710 73 Å). Three standard reflections measured after every 300 reflections showed a decay of 3.54%. The intensity data were corrected for decay and for Lorentz and polarization effects, and empirical absorption corrections based on the ψ-scan of four strong reflections. Crystal and structure determination data for **3** are summarized in Table 1. The centric space group was determined from systematic absences and statistical analysis of intensity distribution and successful refinement of the structure solved by Patterson methods and expanded by Fourier methods¹² and refinement by full-matrix least squares using the software package TeXsan¹³ on a Silicon Graphics Indy computer. A crystallographic asymmetric unit consists of half of the atoms of the complex cation, one molecule of diethyl ether and half a molecule of acetone. 73 H atoms at calculated positions with

TABLE 2: Atomic Coordinates and Thermal Parameters for Non-hydrogen Atoms of 3

atom	<i>x</i>	<i>y</i>	<i>z</i>	<i>B</i> _{eq} ^a , Å ²	atom	<i>x</i>	<i>y</i>	<i>z</i>	<i>B</i> _{eq} ^a , Å ²
Cu(1)	0.02002(3)	0.25185(6)	0.19329(4)	4.43(2)	C(25)	-0.0187(2)	0.3931(5)	0.0097(3)	4.9(2)
Cu(2)	-0.07005(3)	0.27091(6)	0.16489(4)	5.04(2)	C(26)	-0.0263(3)	0.3732(6)	-0.0435(3)	6.3(2)
S(1)	0.0000	0.3043(2)	0.2500	5.91(7)	C(27)	-0.0232(2)	0.2923(6)	-0.0582(3)	6.0(2)
P(1)	0.05418(8)	0.1282(1)	0.20780(9)	5.68(5)	C(28)	-0.0122(3)	0.2305(5)	-0.0158(3)	6.3(2)
P(2)	0.00542(6)	0.3545(1)	0.12619(8)	4.10(4)	C(29)	-0.0042(2)	0.2498(5)	0.0395(3)	5.0(2)
P(3)	-0.09125(6)	0.3580(1)	0.08720(9)	4.63(4)	C(30)	-0.0320(3)	0.2707(8)	-0.1176(4)	9.6(3)
P(4)	-0.11661(7)	0.1737(1)	0.15654(9)	5.12(5)	C(31)	-0.1329(2)	0.4395(5)	0.0659(3)	4.7(2)
P(5)	0.1348(1)	0.1767(2)	-0.1834(1)	9.55(9)	C(32)	-0.1196(2)	0.5109(6)	0.1011(3)	6.1(2)
F(1)	0.1092(3)	0.2610(5)	-0.2050(3)	15.1(3)	C(33)	-0.1508(3)	0.5744(6)	0.0839(4)	7.0(2)
F(2)	0.0918(3)	0.1256(6)	-0.2070(4)	17.2(3)	C(34)	-0.1958(3)	0.5689(6)	0.0329(4)	6.4(2)
F(3)	0.1617(2)	0.0899(5)	-0.1609(3)	13.3(2)	C(35)	-0.2100(2)	0.4952(6)	-0.0008(4)	6.6(2)
F(4)	0.1803(3)	0.2234(6)	-0.1518(4)	17.4(3)	C(36)	-0.1793(2)	0.4315(5)	0.0146(3)	5.9(2)
F(5)	0.1435(3)	0.1868(6)	-0.1196(4)	17.1(3)	C(37)	-0.2287(3)	0.6402(7)	0.0132(4)	8.9(3)
F(6)	0.1272(3)	0.1689(6)	-0.2443(4)	17.7(3)	C(38)	-0.1117(2)	0.3062(5)	0.0160(3)	5.2(2)
O(1)	0.5000	0.0622(9)	0.2500	12.8(4)	C(39)	-0.1260(3)	0.3507(6)	-0.0366(4)	7.0(2)
O(2)	0.6727(4)	0.1037(8)	0.6069(5)	18.3(4)	C(40)	-0.1355(3)	0.3068(8)	-0.0866(4)	9.2(3)
C(1)	-0.0424(2)	0.4205(4)	0.1063(3)	4.4(2)	C(41)	-0.1317(3)	0.2213(8)	-0.0861(5)	9.8(3)
C(2)	0.0868(3)	0.0874(5)	0.2873(3)	5.8(2)	C(42)	-0.1196(3)	0.1792(7)	-0.0360(5)	9.4(3)
C(3)	0.0136(3)	0.0443(5)	0.1607(4)	6.8(2)	C(43)	-0.1090(3)	0.2200(6)	0.0155(4)	7.2(2)
C(4)	-0.0040(4)	0.0359(8)	0.1002(5)	15.2(4)	C(44)	-0.1408(4)	0.1783(10)	-0.1426(5)	14.9(4)
C(5)	-0.0380(4)	-0.0250(9)	0.0618(5)	15.3(4)	C(45)	-0.1551(3)	0.2162(5)	0.1683(3)	5.3(2)
C(6)	-0.0530(4)	-0.0780(7)	0.0809(5)	10.1(3)	C(46)	-0.1493(3)	0.2972(6)	0.1890(3)	6.2(2)
C(7)	-0.0342(4)	-0.0737(9)	0.1380(6)	13.0(4)	C(47)	-0.1766(3)	0.3284(7)	0.2027(4)	7.9(3)
C(8)	-0.0006(4)	-0.0101(8)	0.1780(4)	11.9(4)	C(48)	-0.2110(3)	0.2825(8)	0.1938(4)	8.8(3)
C(9)	-0.0876(4)	-0.1467(8)	0.0398(6)	13.9(4)	C(49)	-0.2180(3)	0.2028(8)	0.1718(4)	8.7(3)
C(10)	0.0944(3)	0.1210(6)	0.1928(3)	6.4(2)	C(50)	-0.1908(3)	0.1685(6)	0.1581(4)	6.9(2)
C(11)	0.1173(4)	0.0468(7)	0.2004(4)	9.8(3)	C(51)	-0.2405(4)	0.318(1)	0.2088(5)	14.2(5)
C(12)	0.1481(4)	0.0480(9)	0.1871(5)	13.1(4)	C(52)	-0.1555(2)	0.1203(5)	0.0821(3)	5.0(2)
C(13)	0.1564(4)	0.119(1)	0.1682(5)	12.5(4)	C(53)	-0.1909(3)	0.1677(6)	0.0321(3)	6.5(2)
C(14)	0.1353(3)	0.1894(8)	0.1611(4)	9.5(3)	C(54)	-0.2201(3)	0.1306(7)	-0.0259(3)	7.1(2)
C(15)	0.1039(3)	0.1911(6)	0.1737(4)	7.1(2)	C(55)	-0.2144(3)	0.0476(7)	-0.0342(3)	6.8(2)
C(16)	0.1923(4)	0.112(1)	0.1573(6)	18.7(6)	C(56)	-0.1787(3)	0.0026(6)	0.0153(4)	7.9(2)
C(17)	0.0526(2)	0.4286(5)	0.1618(3)	4.5(2)	C(57)	-0.1498(3)	0.0384(6)	0.0746(3)	6.3(2)
C(18)	0.0629(2)	0.4822(5)	0.2087(3)	5.5(2)	C(58)	-0.2472(3)	0.0062(8)	-0.0967(4)	10.3(3)
C(19)	0.0997(3)	0.5372(6)	0.2372(3)	6.2(2)	C(59)	0.5000	0.138(1)	0.2500	11.4(5)
C(20)	0.1275(3)	0.5404(5)	0.2210(3)	5.9(2)	C(60)	0.4785(5)	0.186(1)	0.1935(7)	16.4(6)
C(21)	0.1179(2)	0.4865(6)	0.1749(3)	5.7(2)	C(61)	0.7369(7)	0.044(2)	0.6653(9)	24.2(9)
C(22)	0.0811(2)	0.4316(5)	0.1454(3)	4.9(2)	C(62)	0.7245(7)	0.123(2)	0.6358(9)	23.6(9)
C(23)	0.1673(3)	0.6020(7)	0.2526(4)	8.5(3)	C(63)	0.6459(6)	0.136(1)	0.5501(8)	18.9(7)
C(24)	-0.0069(2)	0.3314(5)	0.0534(3)	4.2(2)	C(64)	0.5980(5)	0.1240(10)	0.5192(6)	14.9(5)

$$^a B_{\text{eq}} = \frac{8}{3}\pi^2[U_{11}(aa^*)^2 + U_{22}(bb^*)^2 + U_{33}(cc^*)^2 + 2U_{12}aa^*bb^* \cos \gamma + 2U_{13}aa^*cc^* \cos \beta + 2U_{23}bb^*cc^* \cos \alpha].$$

thermal parameters equal to 1.3 times that of the attached C atoms were not refined. The final agreement factors for **3** are given in Table 1. The final atomic coordinates and thermal parameters for the non-hydrogen atoms are collected in Table 2.

Results and Discussion

Synthesis and Crystal Structure. There have been a number of reports on the various approaches for the synthesis of transition-metal chalcogenide complexes. Examples include those of [Cu₁₂S₈]⁴⁻,^{14a} M₂Ag₆S₄ (M = Na, K),^{14b} [(Ph₃PAu)₄S]-(CF₃SO₃)₂,^{14c} and (Pr₄N)₂[Ag₄(Se₄)₃].^{14d} Fenske and co-workers also demonstrated that (Me₃Si)₂E and its alkyl analogues are useful starting materials for the preparation of transition-metal chalcogenide clusters.^{14e} Similar to the synthesis of **1**, complex **3** was prepared by the reaction between [Cu₂(dtpm)₂(CH₃CN)₂](PF₆)₂ and Na₂S in acetone/methanol. The orange complex gave satisfactory elemental analysis and was characterized by positive FAB-MS and ¹H and ³¹P NMR spectroscopy. The ³¹P NMR spectra revealed a singlet at -11.8, -12.4, and -13.7 ppm for **1**, **2**, and **3**, respectively. The ³¹P signal for **1** which occurred more downfield than that of **2** is in accord with the greater electronegativity of the sulfido ligand. On the other hand, the electron-donating methyl groups on the phenyl rings of the dtpm ligands in **3** render the phosphorus atoms to resonate more upfield.

The structure of [Cu₄(μ-dtpm)₄(μ₄-S)](PF₆)₂ has been established by X-ray crystallography. Figure 1a depicts the perspec-

tive drawing of the complex cation [Cu₄(μ-dtpm)₄(μ₄-S)]²⁺. The [Cu₄S]²⁺ core with the phenyl rings omitted is illustrated in Figure 1b. Selected bond distances and angles are summarized in Table 3. The structure of **3**, similar to other related clusters,^{9a-c} consists of four copper(I) centers arranged in a distorted rectangular array, capped by an unsubstituted μ₄-sulfido ligand with the four dtpm ligands arranged in a two up-two down saddlelike orientation. The Cu-Cu distances in [Cu₄(μ-dtpm)₄(μ₄-S)](PF₆)₂ [2.955(2) and 3.144(2) Å] are slightly longer than those of [Cu₄(μ-dppm)₄(μ₄-S)](PF₆)₂ [2.869(1) and 3.128(1) Å],^{9a} while the Cu-S bond distances [2.233(1) and 2.282(2) Å] are comparable to those of other copper(I) sulfido and thiolato systems.¹⁵

Electronic Absorption and Emission Properties. The electronic absorption spectrum of **3** in CH₃CN (Figure 2a) reveals a high-energy absorption shoulder at ca. 272 nm and a lower energy absorption tail in the 350–450 nm region. Similar absorption patterns have also been observed for complexes **1** and **2**.^{9a,b} The high-energy absorption band is assigned as intraligand IL (dtpm) transition.

Excitation of **3** in the solid state and in fluid solutions at λ > 350 nm results in intense long-lived orange emission. The photophysical data are listed in Table 4. The emission spectrum of **3** in degassed acetone at 298 K is displayed in Figure 2b. The relatively long radiative lifetimes in the microsecond range are suggestive of emissions of a triplet parentage.

Similar to **1** and **2**,^{9a,b} and the isostructural [Ag₄(μ-dppm)₄(μ₄-E)]²⁺ series,^{9c-e} the phosphorescence of **3** is assigned to

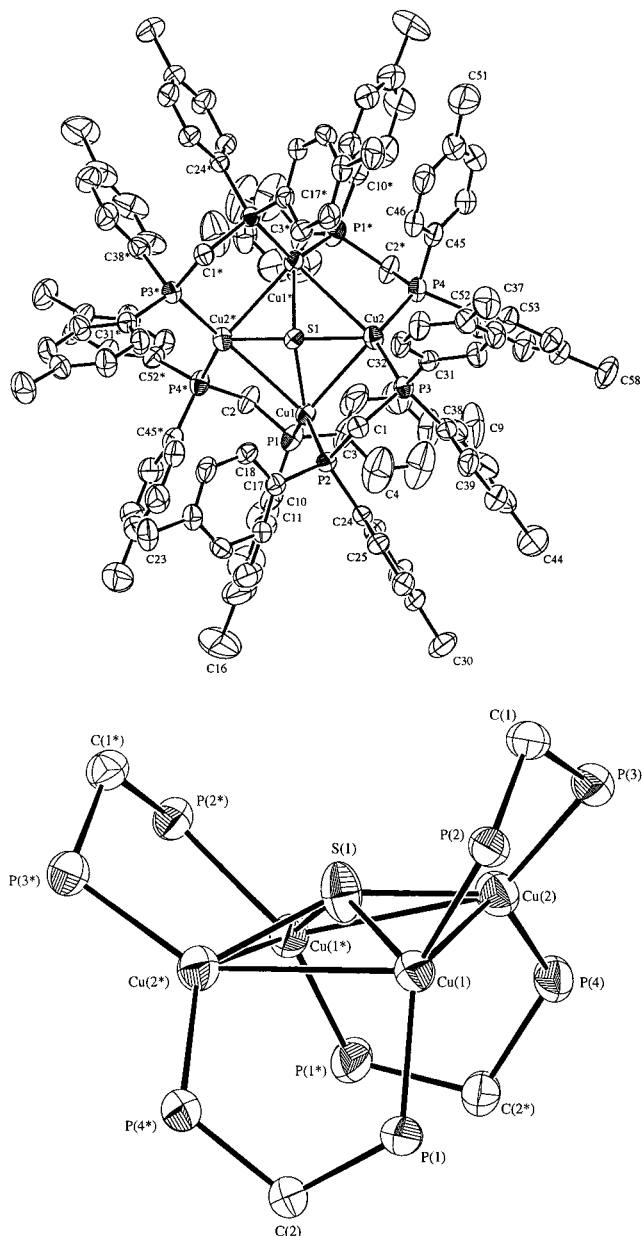


Figure 1. (a, top) Perspective view of the complex cation of **3** with atomic numbering scheme. Thermal ellipsoids are shown at the 35% probability level. (b, bottom) Perspective view of the $[\text{Cu}_4\text{S}]^{2+}$ core of the complex cation of **3** with atomic numbering scheme. The phenyl rings are omitted for clarity. Thermal ellipsoids are shown at the 35% probability level.

TABLE 3: Selected Geometric Data for 3

Selected Bond Lengths (Å)			
Cu(1)–Cu(2)	2.955(2)	Cu(1)–Cu(2*) ^a	3.144(2)
Cu(1)–S(1)	2.282(2)	Cu(2)–S(1)	2.233(1)
Cu(1)–P(1)	2.240(2)	Cu(1)–P(2)	2.272(2)
Cu(2)–P(3)	2.249(2)	Cu(2)–P(4)	2.229(2)
Selected Bond Angles (deg)			
Cu(1)–S(1)–Cu(1*)	137.1(2)	Cu(1)–S(1)–Cu(2)	81.75(6)
Cu(1)–S(1)–Cu(2*)	88.27(7)	Cu(2)–S(1)–Cu(2*)	152.5(2)
S(1)–Cu(1)–P(1)	126.3(1)	S(1)–Cu(1)–P(2)	106.8(1)
S(1)–Cu(2)–P(3)	110.21(10)	S(1)–Cu(2)–P(4)	122.89(8)
P(1)–Cu(1)–P(2)	126.60(10)	P(3)–Cu(2)–P(4)	110.21(10)

^a Starred atoms with coordinates at $(-x, y, \frac{1}{2} - z)$.

originate predominantly from a ligand-to-metal charge-transfer LMCT $[(\text{S}^{2-}) \rightarrow \text{Cu}_4]$ excited state, mixed with a copper(I)-centered (ds/dp) state. Similar assignments have also been suggested in other luminescent polynuclear d^{10} thiolato,^{1a,d,2d,4a,d,5d,7,8j} halo,^{1a–c,e} and alkynyl^{8c,d,f–i,l} systems.

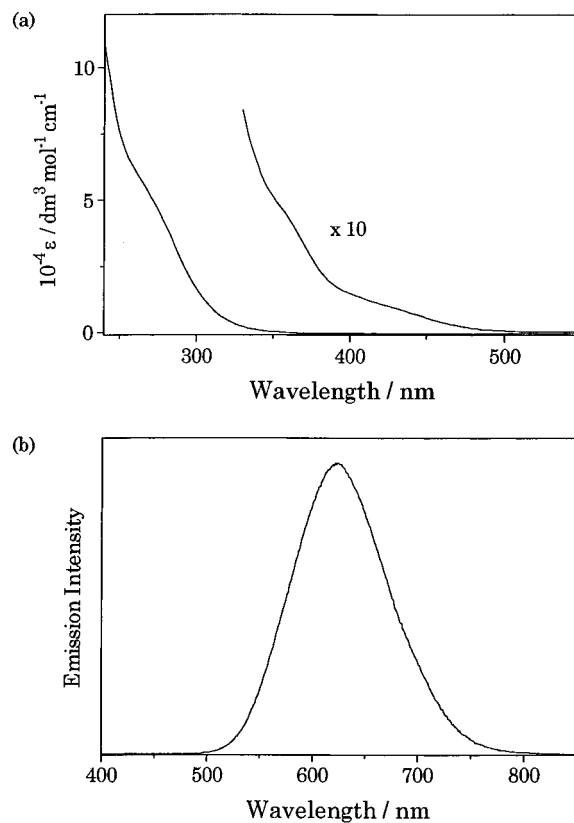


Figure 2. (a) Electronic absorption spectrum of **3** in CH_3CN . (b) Emission spectrum of **3** in degassed acetone at 298 K.

TABLE 4: Photophysical Data

compound	medium (T/K)	emission λ/nm	$\tau_0/\mu\text{s}$	quantum yield Φ^a
1^b	solid (298)	579	3.6 ± 0.1	0.22
	solid (77)	606		
	$(\text{CH}_3)_2\text{CO}$ (298)	622	8.1 ± 0.2	
	CH_3CN (298)	618	7.8 ± 0.2	
2^c	solid (298)	595	3.9 ± 0.2	0.19
	solid (77)	619		
	$(\text{CH}_3)_2\text{CO}$ (298)	626	7.1 ± 0.2	
	CH_3CN (298)	622	6.9 ± 0.2	
3	solid (298)	604	3.5 ± 0.3	0.26
	solid (77)	658		
	$(\text{CH}_3)_2\text{CO}$ (298)	622	8.8 ± 0.4	
	CH_3CN (298)	620	7.7 ± 0.4	

^a In acetone solution. ^b From ref 9a. ^c From ref 9b.

The possibilities that the origin of the emissions being derived from a metal-to-ligand charge-transfer MLCT ($\text{Cu}_4 \rightarrow$ phosphine) or a ligand-to-ligand charge-transfer LLCT $[(\text{S}^{2-}) \rightarrow$ phosphine] transition are excluded, based on the fact that the emission energies of **1**^{9a} and **3** in fluid solutions are almost the same (ca. 620 nm). The presence of an electron-donating methyl group on the dtpm ligand would destabilize its π^* orbital, thereby increasing the MLCT ($\text{Cu}_4 \rightarrow$ phosphine) or LLCT $[(\text{S}^{2-}) \rightarrow$ phosphine] transition energy. However, such an increase in emission energy is not observed and the solid-state emission energy of **1** is even higher than that of the dtpm counterpart **3**, indicating that the π^* of the phosphine ligand is not likely to be the acceptor orbital.

Triplet-State Absorption Spectra. The triplet-state absorption behavior for the complexes **1–3** has been studied with nanosecond transient absorption difference spectroscopy. Figure 3a presents the transient absorption difference spectrum of **1** in degassed acetone following pulse excitation at 355 nm. A plot of $\ln(\Delta A)$ of the triplet-state absorption vs time gives a straight line (Figure 3b), indicating that the decay follows first-order

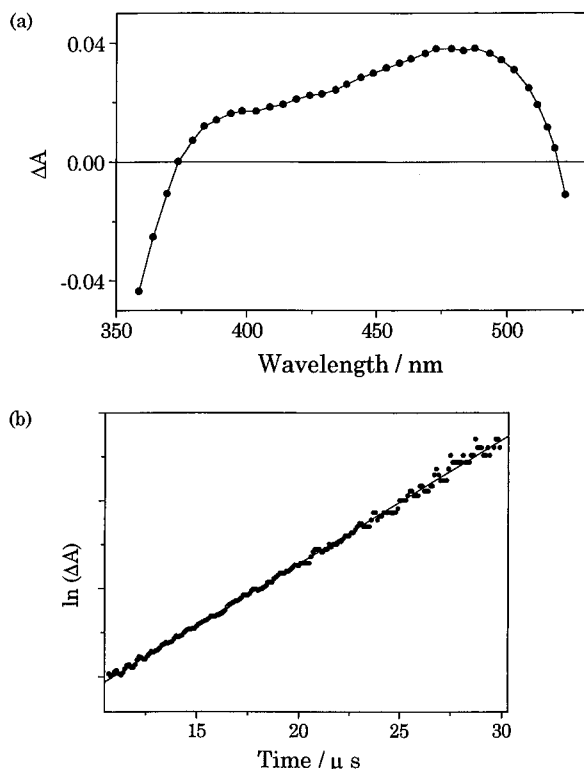


Figure 3. (a) Transient absorption difference spectrum recorded 5 μ s after laser flash for a degassed acetone solution of **1**. (b) Plot of $\ln(\Delta A)$ vs time for the triplet state absorption of **1** at 473 nm.

kinetics. The assignment of the transient absorption as the triplet-state absorption has been confirmed by matching the decay of the transient absorption with that of the phosphorescence. In general, the triplet-state absorption spectra of **1–3** are similar, and are characterized by an absorption shoulder at ca. 380 nm and a structureless absorption extended to a lower energy region (ca. 500 nm). The 480-nm absorption band maximum is most probably an artifact due to the tailing effect of the intense phosphorescence of the complexes at ca. 620 nm. For the same reason, the absorption beyond 520 nm is impossible to record. The origin of the triplet-state absorption bands cannot be assigned with certainty. Similar excited state absorptions have also been observed in the related tetranuclear copper(I) iodide clusters, and the origin has been assigned as a transition from the triplet cluster centered (3CC) state to a higher energy triplet halide-to-ligand charge transfer (3XLCT) state.^{1f}

Electrochemical Properties. Cyclic voltammetric measurements of **3** in CH_3CN (0.1 mol dm^{-3} $n\text{Bu}_4\text{NPF}_6$) revealed four irreversible oxidation waves at ca. +0.29, +0.84, +1.20, and +1.35 V vs Fc^+/Fc , while no reduction waves are detected within the solvent window. Similar observations have also been found for **1**¹⁶ and **2**.^{9b} On the basis of the irreversible nature of the oxidation waves, it appears that the oxidized forms of these copper(I) clusters are unstable within the cyclic voltammetric time scale.

Photochemical Properties. The phosphorescence of **1**^{9a} and **2**^{9b} has been found to be quenched by a series of pyridinium acceptors. The excited-state reduction potentials $E^\circ[\text{Cu}_4(\mu\text{-dppm})_4(\mu_4\text{-E})^{3+/2+*}]$ of $-1.71(10)^{9a}$ and $-1.55(10)^{9b}$ V vs saturated sodium chloride calomel electrode (SSCE) have been estimated for **1** and **2**, respectively. To gain more direct spectroscopic evidence into the mechanism of the photoreactions between these luminescent copper(I) clusters and pyridinium acceptors, a nanosecond transient absorption spectroscopic study has been carried out. Complex **1** has been found to be quenched by 4-(methoxycarbonyl)-*N*-methylpyridinium hexafluorophosphate with a bimolecular quenching rate constant, k_q of $3.35 \times$

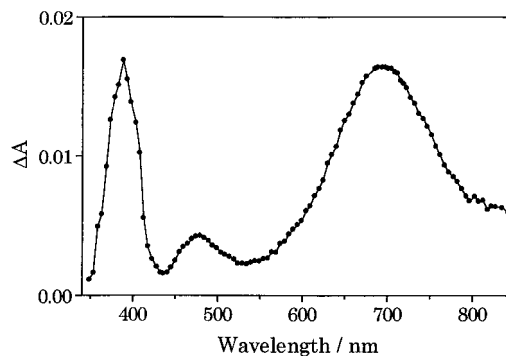
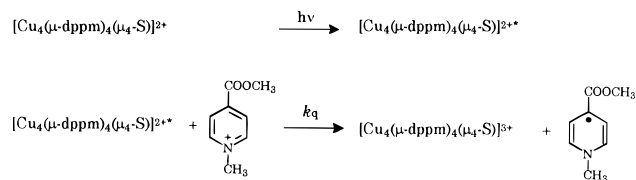


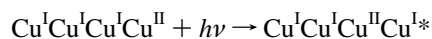
Figure 4. Transient absorption difference spectrum recorded 10 μ s after laser flash for the reaction of **1*** and 4-(methoxycarbonyl)-*N*-methylpyridinium in degassed acetone.

$10^9 \text{ dm}^3 \text{ mol}^{-1} \text{ s}^{-1}$.^{9a} The transient absorption difference spectrum of a degassed acetone solution of **1** ($0.27 \times 10^{-3} \text{ mol dm}^{-3}$) and 4-(methoxycarbonyl)-*N*-methylpyridinium hexafluorophosphate ($7.93 \times 10^{-3} \text{ mol dm}^{-3}$) is shown in Figure 4. A sharp absorption band is observed at approximately 390 nm, concomitant with the formation of a lower intensity band at ca. 484 nm and a more intense broad absorption band at ca. 693 nm. The high-energy absorption band at ca. 390 nm is characteristic of the pyridinyl radical and matches well with the reported spectrum of the 4-(methoxycarbonyl)-*N*-methylpyridinyl radical.¹⁷ The reaction mechanism is likely to be:



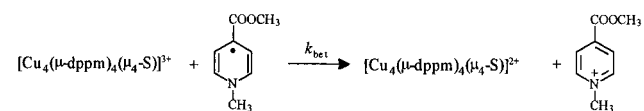
The 484-nm band and the intense broad absorption at ca. 693 nm are not typical of the pyridinyl radical but should be characteristic of the one-electron oxidized form of the cluster, $[\text{Cu}^{\text{I}}\text{Cu}^{\text{I}}\text{Cu}^{\text{I}}\text{Cu}^{\text{II}}(\mu\text{-dppm})_4(\mu_4\text{-S})]^{3+}$. Although ligand-field ($d-d$) transitions for a copper(II) metal center in an unsymmetric environment can occur at such a low-energy region,¹⁸ such an assignment for both the 484- and 693-nm absorption bands is not favored, given the relatively high extinction coefficients of ca. 1200 and 6700 $\text{dm}^3 \text{ mol}^{-1} \text{ cm}^{-1}$ estimated, respectively, on the assumption that both **1** and **1**⁺ do not have significant absorption at ca. 390 nm. Another possible assignment is the ligand-to-metal charge-transfer LMCT [$(\text{S}^{2-}) \rightarrow \text{Cu}(\text{II})$] transition, which is commonly suggested in many mixed-valence copper(I,II) thiolate complexes. For example, the absorption band at ca. 518 nm observed in $\text{Cu}_4^{\text{I}}\text{Cu}_2^{\text{II}}[\text{SC}(\text{CH}_3)_2\text{CH}_2\text{NH}_2]_{12}\text{-Cl}$ and related thiolate clusters has been assigned to be a LMCT [$(\text{S}^{2-}) \rightarrow \text{Cu}(\text{II})$] transition;¹⁹ the extinction coefficient of which [$3400 \text{ dm}^3 \text{ mol}^{-1} \text{ cm}^{-1}$ per Cu(II)] is comparable to that of the 484-nm band observed in the transient absorption difference spectrum. Similar assignment has also been suggested for the absorption bands at 400–500 nm of a series of copper(II) complexes with thioethers as ligands.²⁰ However, such an assignment for the broad absorption at 693 nm is less likely in view of its occurrence at such a low-energy region.

With reference to our previous transient absorption spectroscopic work on photoinduced electron-transfer reactions between a series of trinuclear alkynylcopper(I) complexes and pyridinium acceptors and the observation of a mixed-valence copper species in the transient absorption spectra in the near-infrared region,^{8d,h} an assignment of the 693-nm transient absorption as an intervalence-transfer (IT) transition is likely:



Similar intervalence-transfer transitions have also been reported in a variety of mixed-valence copper(I,II) systems. An example is the dinuclear macrocyclic complex $[\text{Cu}^{\text{I}}\text{Cu}^{\text{II}}\text{L}]^{3+}$ [$\text{L} = \text{N}(\text{CH}_2\text{CH}_2\text{N}=\text{C}=\text{C}=\text{NCH}_2\text{CH}_2)_3\text{N}$] which shows an intervalence-transfer (IT) band at 756 nm ($\epsilon = 5000 \text{ dm}^3 \text{ mol}^{-1} \text{ cm}^{-1}$).²¹ Similar assignment has also been suggested in other mixed-valence Cu(I)Cu(II) systems with thiolato,^{22a} halo,^{22b,c} or *N,O*-containing macrocyclic ligands.^{22d,e}

The transient absorptions are found to decay with time. A decay trace of the 693-nm absorption is shown in Figure 5a. A plot of $(1/\Delta A)$ vs time gives a straight line (Figure 5b), indicating that the decay follows second-order kinetics, corresponding to the back electron-transfer reaction:



A back electron-transfer rate constant k_{bet} of $9.7 \times 10^9 \text{ dm}^3 \text{ mol}^{-1} \text{ s}^{-1}$ is determined based on the decay of the mixed valence species from the equation

$$k_{\text{bet}} = b \times m \times \Delta\epsilon$$

where b is the path length of the optical cell, m is the slope of the straight line obtained from the plot $(1/\Delta A)$ vs time, and $\Delta\epsilon = \sum\epsilon(\text{products}) - \sum\epsilon(\text{reactants})$. This value agrees well with that obtained from the pyridinyl radical decay trace.

Similarly, complex **1** is quenched by 4-(aminoformyl)-*N*-methylpyridinium hexafluorophosphate with a k_q of $1.77 \times 10^9 \text{ dm}^3 \text{ mol}^{-1} \text{ s}^{-1}$.^{9a} Transient absorptions have also been observed for the photoinduced electron-transfer reactions between **1*** and 4-(aminoformyl)-*N*-methylpyridinium, and methylviologen hexafluorophosphates, respectively. For the case of 4-(aminoformyl)-*N*-methylpyridinium acceptor, a sharp absorption peak at ca. 390 nm, a less intense peak at 475 nm, and a broad and intense band at 690 nm are observed. Similarly, the highest energy band is in accord with the characteristic absorption of the pyridinyl radical,¹⁷ and the lower energy 475-nm peak and the broad band at ca. 690 nm are assigned as ligand-to-metal charge-transfer LMCT [$(\text{S}^{2-}) \rightarrow \text{Cu}(\text{II})$] and intervalence-transfer IT transitions of the mixed-valence $\text{Cu}^{\text{I}}\text{Cu}^{\text{I}}\text{Cu}^{\text{I}}\text{Cu}^{\text{II}}$ species, respectively. A k_{bet} value of $2.2 \times 10^{10} \text{ dm}^3 \text{ mol}^{-1} \text{ s}^{-1}$ is estimated. The smaller k_q and larger k_{bet} values observed with 4-(aminoformyl)-*N*-methylpyridinium acceptor than 4-(methoxycarbonyl)-*N*-methylpyridinium are in line with the more negative reduction potential of the former, leading to a less negative ΔG° for the forward reaction and a more negative ΔG° for the back electron-transfer step, consistent with that predicted for the normal region according to Marcus theory. For the case with methylviologen, characteristic absorptions at ca. 390 and 605 nm, typical of the methylviologen cation radical are observed.²³ The absorptions of the mixed-valence $\text{Cu}^{\text{I}}\text{Cu}^{\text{I}}\text{Cu}^{\text{I}}\text{Cu}^{\text{II}}$ species appear to be obscured by the intense absorption of $\text{MV}^{+\cdot}$.

Similarly, transient absorption difference spectra have also been obtained for the electron-transfer reactions between **2*** and 4-(methoxycarbonyl)-*N*-methylpyridinium (Figure 6), 4-(aminoformyl)-*N*-methylpyridinium, and methylviologen hexafluorophosphates, respectively. The broad intense absorption at 685 nm has also been assigned as the absorption of the mixed-valence $\text{Cu}^{\text{I}}\text{Cu}^{\text{I}}\text{Cu}^{\text{I}}\text{Cu}^{\text{II}}$ species of **2**⁺. The occurrence of the 685-nm absorption at similar energy as that of the sulfido analogue **1** (693 nm) further excludes their assignments as LMCT transitions where a much lower energy absorption would

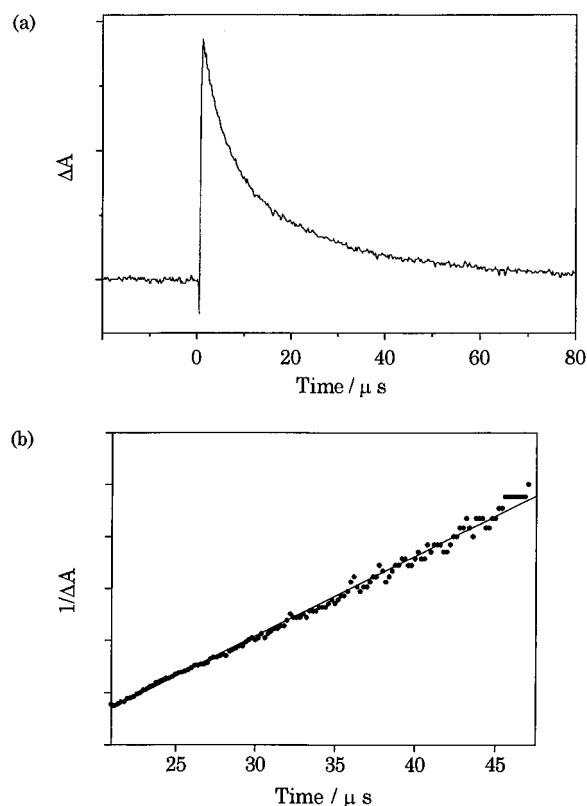


Figure 5. (a) Decay trace of mixed-valence species $[\text{Cu}^{\text{I}}\text{Cu}^{\text{I}}\text{Cu}^{\text{I}}\text{Cu}^{\text{II}}-(\mu\text{-dppm})_4(\mu_4\text{-S})]^{3+}$ at 693 nm for the reaction of **1*** and 4-(methoxycarbonyl)-*N*-methylpyridinium in degassed acetone. (b) Plot of $(1/\Delta A)$ vs time at 693 nm.

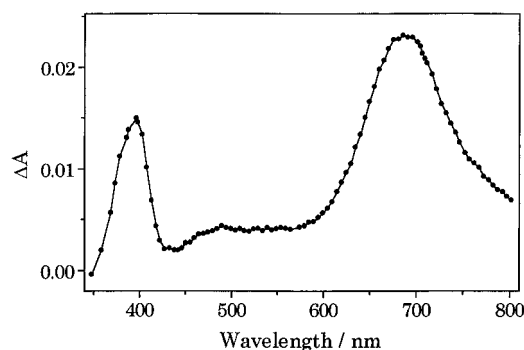


Figure 6. Transient absorption difference spectrum recorded 10 μs after laser flash for the reaction of **2*** and 4-(methoxycarbonyl)-*N*-methylpyridinium in degassed acetone.

be expected for the selenido than the sulfido analogue. Instead, an assignment of intervalence-transfer transition appears to be more likely for these low-energy absorptions. The back electron-transfer rate constants between the oxidized species **2**⁺ and the reduced 4-(methoxycarbonyl)-*N*-methylpyridinyl and 4-(aminoformyl)-*N*-methylpyridinyl radicals are estimated to be 1.4×10^{10} and $2.4 \times 10^{10} \text{ dm}^3 \text{ mol}^{-1} \text{ s}^{-1}$, respectively, also in line with those predicted according to Marcus theory.

For **3**, similar photoinduced electron-transfer reactions with different pyridinium acceptors have also been found to occur. The transient absorption difference spectrum of a degassed acetone solution of **3** and 4-(methoxycarbonyl)-*N*-methylpyridinium hexafluorophosphate is depicted in Figure 7. In general, all the spectra are very similar to those of the dppm analogue **1**, indicative of relatively little participation of the bridging phosphine ligand in the absorption characteristics of the transient species. Similar to those of complexes **1** and **2**, the back electron-transfer rate constants between the oxidized species **3**⁺ and reduced 4-(methoxycarbonyl)-*N*-methylpyridinyl and 4-(ami-

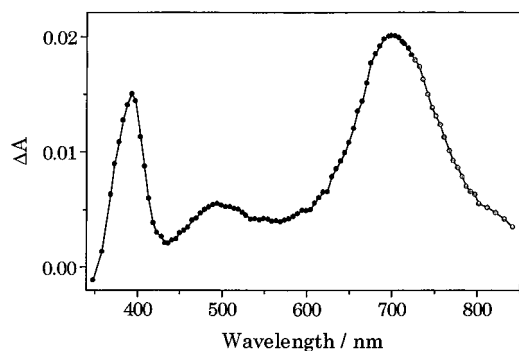


Figure 7. Transient absorption difference spectrum recorded 10 μ s after laser flash for the reaction of 3^* and 4-(methoxycarbonyl)-*N*-methylpyridinium in degassed acetone.

noformyl)-*N*-methylpyridinyl radicals are estimated to be 9.7×10^9 and $2.1 \times 10^{10} \text{ dm}^3 \text{ mol}^{-1} \text{ s}^{-1}$, respectively.

In conclusion, characteristic pyridinyl radical absorptions have been observed in all transient absorption difference spectra studied, thus providing direct spectroscopic evidence for the electron-transfer nature of the photoreactions between the phosphorescent states of these tetranuclear copper(I) chalcogenide clusters and the pyridinium acceptors. The highly reducing capabilities of the excited states of these copper(I) clusters have also been demonstrated.

Acknowledgment. V.W.-W.Y. acknowledges financial support from the Research Grants Council and The University of Hong Kong, K.K.-W.L. the receipt of a Sir Edward Youde Postgraduate Fellowship, administered by the Sir Edward Youde Memorial Fund Council, and a Postgraduate Studentship, administered by The University of Hong Kong, and C.-R.W. the receipt of a Postdoctoral Fellowship, also administered by The University of Hong Kong.

Supporting Information Available: Text giving details of crystal structure solution and tables giving fractional coordinates and thermal parameters for all atoms, general displacement parameter expressions U , and complete lists of bond distances and bond angles (17 pages); observed and calculated structure factors (33 pages). Ordering information is given on any current masthead page.

References and Notes

- (1) (a) Ford, P. C.; Vogler, A. *Acc. Chem. Res.* **1993**, *26*, 220. (b) Kyle, K. R.; Ryu, C. K.; DiBenedetto, J. A.; Ford, P. C. *J. Am. Chem. Soc.* **1991**, *113*, 2954. (c) Vitale, M.; Palke, W. E.; Ford, P. C. *J. Phys. Chem.* **1992**, *96*, 8329. (d) Sabin, F.; Ryu, C. K.; Ford, P. C.; Vogler, A. *Inorg. Chem.* **1992**, *31*, 1941. (e) Ford, P. C. *Coord. Chem. Rev.* **1994**, *132*, 129. (f) Lindsay, E.; Ford, P. C. *Inorg. Chim. Acta* **1996**, *242*, 51.
- (2) (a) Vogler, A.; Kunkely, H. *J. Am. Chem. Soc.* **1986**, *108*, 7211. (b) Vogler, A.; Kunkely, H. *Chem. Phys. Lett.* **1988**, *150*, 135. (c) Vogler, A.; Kunkely, H. *Chem. Phys. Lett.* **1989**, *158*, 74. (d) Kunkely, H.; Vogler, A. *Chem. Phys. Lett.* **1989**, *164*, 621. (e) Kunkely, H.; Vogler, A. *J. Chem. Soc., Chem. Commun.* **1990**, 1204.
- (3) (a) Caspar, J. V. *J. Am. Chem. Soc.* **1985**, *107*, 6718. (b) Harvey, P. D.; Gray, H. B. *J. Am. Chem. Soc.* **1988**, *110*, 2145. (c) Harvey, P. D.; Schaefer, W. P.; Gray, H. B. *Inorg. Chem.* **1988**, *27*, 1101.
- (4) (a) Avdeef, A.; Fackler, J. P., Jr. *Inorg. Chem.* **1978**, *17*, 2182. (b) Khan, Md. N. I.; Fackler, J. P., Jr.; King, C.; Wang, J. C.; Wang, S. *Inorg. Chem.* **1988**, *27*, 1672. (c) King, C.; Wang, J. C.; Khan, Md. N. I.; Fackler, J. P., Jr. *Inorg. Chem.* **1989**, *28*, 2145. (d) Forward, J. M.; Bohmann, D.; Fackler, J. P., Jr.; Staples, R. J. *Inorg. Chem.* **1995**, *34*, 6330.
- (5) (a) Barrie, J. D.; Dunn, B.; Hollingsworth, G.; Zink, J. I. *J. Phys. Chem.* **1989**, *93*, 3958. (b) Shin, K. S. K.; Barrie, J. D.; Dunn, B.; Zink, J. I. *J. Am. Chem. Soc.* **1990**, *112*, 5701. (c) Henary, M.; Zink, J. I. *Inorg. Chem.* **1991**, *30*, 3111. (d) Hanna, S. D.; Zink, J. I. *Inorg. Chem.* **1996**, *35*, 297.
- (6) (a) Che, C. M.; Kwong, H. L.; Yam, V. W. W.; Cho, K. C. *J. Chem. Soc., Chem. Commun.* **1989**, 885. (b) Che, C. M.; Kwong, H. L.; Poon, C. K.; Yam, V. W. W. *J. Chem. Soc., Dalton Trans.* **1990**, 3215. (c) Che, C. M.; Yip, H. K.; Li, D.; Peng, S. M.; Lee, G. H.; Wang, Y. M.; Liu, S. T. *J. Chem. Soc., Chem. Commun.* **1991**, 1615. (d) Che, C. M.; Yip, H. K.; Yam, V. W. W.; Cheung, P. Y.; Lai, T. F.; Shieh, S. J.; Peng, S. M. *J. Chem. Soc., Dalton Trans.* **1992**, 427. (e) Che, C. M.; Yip, H. K.; Lo, W. C.; Peng, S. M. *Polyhedron* **1994**, *13*, 887. (f) Hong, X.; Cheung, K. K.; Guo, C. X.; Che, C. M. *J. Chem. Soc., Dalton Trans.* **1994**, 1867.
- (7) (a) Jones, W. B.; Yuan, J.; Narayanaswamy, R.; Young, M. A.; Elder, R. C.; Bruce, A. E.; Bruce, M. R. M. *Inorg. Chem.* **1995**, *34*, 1996. (b) Narayanaswamy, R.; Young, M. A.; Parkhurst, E.; Ouellette, M.; Kerr, M. E.; Ho, D. M.; Elder, R. C.; Bruce, A. E.; Bruce, M. R. M. *Inorg. Chem.* **1993**, *32*, 2506. (c) Knotter, D. M.; Blasse, G.; van Vliet, J. P. M.; van Koten, G. *Inorg. Chem.* **1992**, *31*, 2196.
- (8) (a) Yam, V. W. W.; Lai, T. F.; Che, C. M. *J. Chem. Soc., Dalton Trans.* **1990**, 3747. (b) Yam, V. W. W.; Lee, W. K. *J. Chem. Soc., Dalton Trans.* **1993**, 2097. (c) Yam, V. W. W.; Lee, W. K.; Lai, T. F. *Organometallics* **1993**, *12*, 2383. (d) Yam, V. W. W.; Lee, W. K.; Yeung, P. K. Y.; Phillips, D. *J. Phys. Chem.* **1994**, *98*, 7545. (e) Yam, V. W. W.; Choi, S. W. K. *J. Chem. Soc., Dalton Trans.* **1994**, 2057. (f) Yam, V. W. W.; Fung, W. K. M.; Cheung, K. K. *Angew. Chem., Int. Ed. Engl.* **1996**, *35*, 1100. (g) Yam, V. W. W.; Lee, W. K.; Cheung, K. K. *J. Chem. Soc., Dalton Trans.* **1996**, 2335. (h) Yam, V. W. W.; Lee, W. K.; Cheung, K. K.; Crystall, B.; Phillips, D. *J. Chem. Soc., Dalton Trans.* **1996**, 3283. (i) Yam, V. W. W.; Lee, W. K.; Cheung, K. K.; Lee, H. K.; Leung, W. P. *J. Chem. Soc., Dalton Trans.* **1996**, 2889. (j) Yam, V. W. W.; Chan, C. L.; Cheung, K. K. *J. Chem. Soc., Dalton Trans.* **1996**, 4019. (k) Yam, V. W. W.; Choi, S. W. K.; Cheung, K. K. *Organometallics* **1996**, *15*, 1734. (l) Yam, V. W. W.; Choi, S. W. K.; Chan, C. L.; Cheung, K. K. *Chem. Commun.* **1996**, 2067. (m) Yam, V. W. W.; Choi, S. W. K. *J. Chem. Soc., Dalton Trans.* **1996**, 4227.
- (9) (a) Yam, V. W. W.; Lee, W. K.; Lai, T. F. *J. Chem. Soc., Chem. Commun.* **1993**, 1571. (b) Yam, V. W. W.; Lo, K. K. W.; Cheung, K. K. *Inorg. Chem.* **1996**, *35*, 3459. (c) Yam, V. W. W.; Lo, K. K. W.; Wang, C. R.; Cheung, K. K. *Inorg. Chem.* **1996**, *35*, 5116. (d) Wang, C. R.; Lo, K. K. W.; Yam, V. W. W. *J. Chem. Soc., Dalton Trans.* **1997**, 227. (e) Wang, C. R.; Lo, K. K. W.; Yam, V. W. W. *Chem. Phys. Lett.* **1996**, *262*, 91.
- (10) (a) Ziegler, C. B., Jr.; Heck, R. F. *J. Org. Chem.* **1978**, *43*, 2941. (b) Kubas, G. J. *Inorg. Synth.* **1979**, *19*, 90. (c) Perrin, D. D.; Armarego, W. L. F.; Perrin, D. R. *Purification of Laboratory Chemicals*, 2nd ed.; Pergamon: Oxford, U.K., 1980. (d) Aguiar, A. M.; Beisler, J. *J. Org. Chem.* **1964**, *29*, 1660. (e) Diez, J.; Gamasa, M. P.; Gimeno, J.; Tiripicchio, A.; Camellini, M. T. *J. Chem. Soc., Dalton Trans.* **1987**, 1275.
- (11) Demas, J. N.; Crosby, G. A. *J. Phys. Chem.* **1971**, *75*, 991.
- (12) *PATY* and *DIRDIF92*: Beurskens, P. T.; Admiraal, G.; Beurskens, G.; Bosman, W. P.; Garcia-Granda, S.; Gould, R. O.; Smits, J. M. M.; Smykalla, C.; 1992. The *DIRDIF* program system, Technical Report of the Crystallography Laboratory, University of Nijmegen, The Netherlands.
- (13) *TeXsan*: Crystal Structure Analysis Package, Molecular Structure Corp., 1985, 1992.
- (14) (a) Betz, P.; Krebs, B.; Henkel, G. *Angew. Chem., Int. Ed. Engl.* **1984**, *23*, 311. (b) Wood, P. T.; Pennington, W. T.; Kolis, J. W. *J. Chem. Soc., Chem. Commun.* **1993**, 235. (c) Canales, F.; Gimeno, M. C.; Jones, P. G.; Laguna, A. *Angew. Chem., Int. Ed. Engl.* **1994**, *33*, 769. (d) Huang, S. P.; Kanatzidis, M. G. *Inorg. Chem.* **1991**, *30*, 1455. (e) Fenske, D. *Clusters and Colloids: From Theory to Applications*; Schmid, G., Ed.; VCH, Weinheim, Germany, 1994, 231.
- (15) (a) Dehnen, S.; Schäfer, A.; Fenske, D.; Ahlrichs, R. *Angew. Chem., Int. Ed. Engl.* **1994**, *33*, 746. (b) Coucouvanis, D.; Murphy, C. N.; Kanodia, S. K. *Inorg. Chem.* **1980**, *19*, 2993.
- (16) Yam, V. W. W.; Lee, W. K., unpublished results.
- (17) Hermolin, J.; Levin, M.; Kosower, E. M. *J. Am. Chem. Soc.* **1981**, *103*, 4808.
- (18) Lever, A. B. P. *Inorganic Electronic Spectroscopy*, 2nd ed.; Elsevier: Amsterdam, The Netherlands, 1984.
- (19) (a) Schugar, H. J.; Ou, C.; Thich, J. A.; Potenza, J. A.; Lalancette, R. A.; Furey, W., Jr. *J. Am. Chem. Soc.* **1976**, *98*, 3047. (b) Birker, P. J. M. W. L. *Inorg. Chem.* **1979**, *18*, 3502. (c) Schugar, H. J.; Ou, C.; Thich, J. A.; Potenza, J. A.; Felthouse, T. R.; Haddad, M. S.; Hendrickson, D. N.; Furey, W. F., Jr.; Lalancette, R. A. *Inorg. Chem.* **1980**, *19*, 543. (d) Birker, P. J. M. W. L.; Freeman, H. C. *J. Am. Chem. Soc.* **1977**, *99*, 6890.
- (20) (a) Miskowski, V. M.; Thich, J. A.; Solomon, R.; Schugar, H. J. *J. Am. Chem. Soc.* **1976**, *98*, 8344. (b) Ainscough, E. W.; Brodie, A. M.; Husbands, J. M.; Gainsford, G. J.; Gabe, E. J.; Curtis, N. F. *J. Chem. Soc., Dalton Trans.* **1985**, 151.
- (21) Barr, M. E.; Smith, P. H.; Antholine, W. E.; Spencer, B. *J. Chem. Soc., Chem. Commun.* **1993**, 1649.
- (22) (a) Robin, M. B.; Day, P. *Adv. Inorg. Chem. Radiochem.* **1967**, *10*, 247. (b) Delsahüt, I. S.; Loeb, B. L. *J. Coord. Chem.* **1994**, *33*, 33. (c) Scott, B.; Willett, R.; Porter, L.; Williams, J. *Inorg. Chem.* **1992**, *31*, 2483. (d) Gagné, R. R.; Koval, C. A.; Smith, T. J. *J. Am. Chem. Soc.* **1977**, *99*, 8367. (e) Gagné, R. R.; Koval, C. A.; Smith, T. J.; Cimolino, M. C. *J. Am. Chem. Soc.* **1979**, *101*, 4571.
- (23) Watanabe, T.; Honda, K. *J. Phys. Chem.* **1982**, *86*, 2617.